

Dense Siamese Network

Wenwei Zhang¹ Jiangmiao Pang^{2,4} Kai Chen^{3,4} Chen Change Loy¹✉

¹S-Lab, Nanyang Technological University

²CUHK-SenseTime Joint Lab, the Chinese University of Hong Kong

³SenseTime Research ⁴Shanghai AI Laboratory

{wenwei001, ccloy}@ntu.edu.sg pangjiangmiao@gmail.com
chenkai@sensetime.com

Abstract

This paper presents Dense Siamese Network (DenseSiam), a simple unsupervised learning framework for dense prediction tasks. It learns visual representations by maximizing the similarity between two views of one image with two types of consistency, i.e., pixel consistency and region consistency. Concretely, DenseSiam first maximizes the pixel level spatial consistency according to the exact location correspondence in the overlapped area. It also extracts a batch of region embeddings that correspond to some sub-regions in the overlapped area to be contrasted for region consistency. In contrast to previous methods that require negative pixel pairs, momentum encoders or heuristic masks, DenseSiam benefits from the simple Siamese network and optimizes the consistency of different granularities. It also proves that the simple location correspondence and interacted region embeddings are effective enough to learn the similarity. We apply DenseSiam on ImageNet and obtain competitive improvements on various downstream tasks. We also show that only with some extra task-specific losses, the simple framework can directly conduct dense prediction tasks. On an existing unsupervised semantic segmentation benchmark, it surpasses state-of-the-art segmentation methods by 2.1 mIoU with 28% training costs.

1. Introduction

Dense prediction tasks, such as image segmentation and object detection, are fundamental computer vision tasks with many real-world applications. Beyond conventional supervised learning methods, recent research interests grow in unsupervised learning to train networks from large-scale unlabeled datasets. These methods either learn representations as pre-trained weights then fine-tune on downstream tasks [10, 51] or directly learn for specific tasks [11].

In recent years, unsupervised pre-training has attracted a

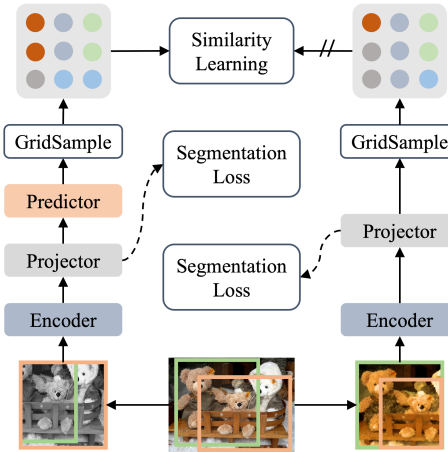


Figure 1. **Dense Siamese Network** (DenseSiam) unanimously solves unsupervised pre-training and unsupervised semantic segmentation. The pair of images are first processed by the same encoder network and a convolutional projector. Then a predictor is applied on one side, and a stop-gradient operation on the other side. A grid sampling method is used to extract dense predictions in the overlapped area. DenseSiam can perform unsupervised semantic segmentation by simply adding a segmentation loss.

lot of attention. Much effort has been geared to learn global representation for image classification [6, 8, 10, 19, 20]. As the global average pooling in these methods discards spatial information, it has been observed [6, 8, 19, 51] that the learned representations are sub-optimal for dense uses. Naturally, some attempts conduct similarity learning at pixel-level [35, 45, 50] or region-level [24, 37, 40, 48, 49] and maintain the main structures in global ones to learn representations for dense prediction tasks.

Despite the remarkable progress in that field, the development in unsupervised learning for specific tasks is relatively slow-moving. For example, solutions in unsupervised semantic segmentation [11, 27, 33] rely more on clustering methods (such as k-means) that are also derived from unsupervised image classification [5, 6, 27]. When reflecting

on these similar tasks from the perspective of unsupervised learning, we observe these tasks share the inherent goal of maximizing the similarity of dense predictions (either labels or embeddings) across images but differ in the task-specific training objectives.

In this paper, we propose *Dense Siamese Network* (DenseSiam) to unanimously solve these dense unsupervised learning tasks within a single framework (Fig. 1). It learns visual representations by maximizing two types of consistency, *i.e.*, pixel consistency and region consistency, with methods dubbed as *PixSim* and *RegionSim*, respectively. The encoder here can be directly fine-tuned for various downstream dense prediction tasks after unsupervised pre-training. By adding an extra segmentation loss to the projector and setting its channel number consistent with the number of categories in the dataset, the encoder and projector is capable of learning class-wise representations for unsupervised semantic segmentation.

Specifically, PixSim learns to maximize the pixel-level spatial consistency between the grid sampled predictions. Its training objective is constrained under the exact location correspondence. In addition, the projected feature maps are multiplied with the features from encoder to generate a batch of region embeddings on each image, where each region embedding corresponds to a sub-region in the overlapped area. RegionSim then conducts contrastive learning between pairs of region embeddings and optimizes them to be consistent.

In contrast to previous unsupervised pre-training methods for dense prediction tasks, DenseSiam benefits from the simple Siamese network [10] that does not have negative pixel pairs [45, 50] and momentum encoders [37, 50]. Uniquely, DenseSiam optimizes the consistency of different granularities. The optimization for each granularity is simple as it neither requires heuristic masks [24] nor manual regions crops [37, 48, 49].

Extensive experiments show that DenseSiam is capable of learning strong representation for dense prediction tasks. DenseSiam obtains nontrivial 0.4 AP^{mask}, 0.7 mIoU, and 1.7 AP improvement in comparison with SimSiam when transferring its representation on COCO instance segmentation, Cityscapes semantic segmentation, and PASCAL VOC detection, respectively. For unsupervised semantic segmentation, DenseSiam makes the first attempt to discard clustering [11, 27] while surpassing previous state-of-the-art method [11] by **2.1** mIoU with only \sim 28% of the original training costs.

2. Related Work

Siamese Network. Siamese network [3] was proposed for comparing entities. They have many applications including object tracking [2], face verification [39, 41], and one-shot recognition [28]. In conventional use cases, Siamese

Table 1. **Comparison of unsupervised dense representation learning methods.** ‘Heu.’ is abbreviation of heuristic, indicating whether heuristic mask or saliency map is used

Method	Base	Pixel	Region	Heu.	Correspondence
DenseCL [45]	MoCo v2 [9]	✓	✗	✗	feature similarity
PixPro [50]	SimCLR [8]	✓	✗	✗	coordinate distance
VaDER [35]	MoCo v2	✓	✗	✗	location
ReSim [48]	MoCo v2	✗	✓	✗	dense region crops
SCRL [37]	BYOL [19]	✗	✓	✗	sampled region crops
DetCo [49]	MoCo v2	✗	✓	✗	image patches
DetCon [24]	SimCLR [8]	✗	✓	✓	heuristic masks
CAST [40]	MoCo v2	✗	✓	✓	saliency map
DenseSiam	SimSiam [10]	✓	✓	✗	location + region embeddings

Network takes different images as input and outputs either a global embedding of each image for comparison [3, 28, 39, 41] or outputs feature map of each image for cross-correlation [2]. DenseSiam uses the Siamese architecture to output pixel embeddings and maximizes similarity between embeddings of the same pixel from two views of an image to pre-train dense representations with strong transferability in dense prediction tasks.

Unsupervised Representation Learning. Representative unsupervised representation learning methods include contrastive learning [1, 8, 9, 15, 20, 47] and clustering-based methods [5, 6, 43, 52]. Notably, Siamese network has become a common structure in recent attempts [6, 8, 19], despite their different motivations and solutions to avoid the feature ‘collapsing’ problem. SimSiam [10] studies the minimum core architecture in these methods [6, 8, 19] and shows that a simple Siamese network with stopping gradient can avoid feature ‘collapsing’ and yield strong representations.

Given the different natures of image-level representation learning and dense prediction tasks, more recent attempts [14, 24, 35, 37, 40, 45, 48–51] pre-train dense representations specially designed for dense prediction tasks. Most of these methods conduct similarity learning with pixels [35, 45, 50], manually cropped patches of image or features [37, 48, 49], and regional features segmented by saliency map [40] or segmentation masks [24] obtained in unsupervised manners. These methods still need a momentum encoder [35, 37, 45, 49, 50] or negative pixel samples [35, 45, 50], although they [8, 19] have been proven unnecessary [10] in image-level representation learning.

DenseSiam only needs a Siamese network with a stop gradient operation to obtain strong dense representations, without momentum encoder [35, 37, 45, 49, 50] nor negative pixel pairs [35, 45, 50] (Table 1). It conducts contrastive learning among regional features inside an image emerged via pixel similarity learning. Thanks for the unique design, DenseSiam performs region-level similarity learning without saliency maps [40], region crops [37, 48, 49], nor seg-

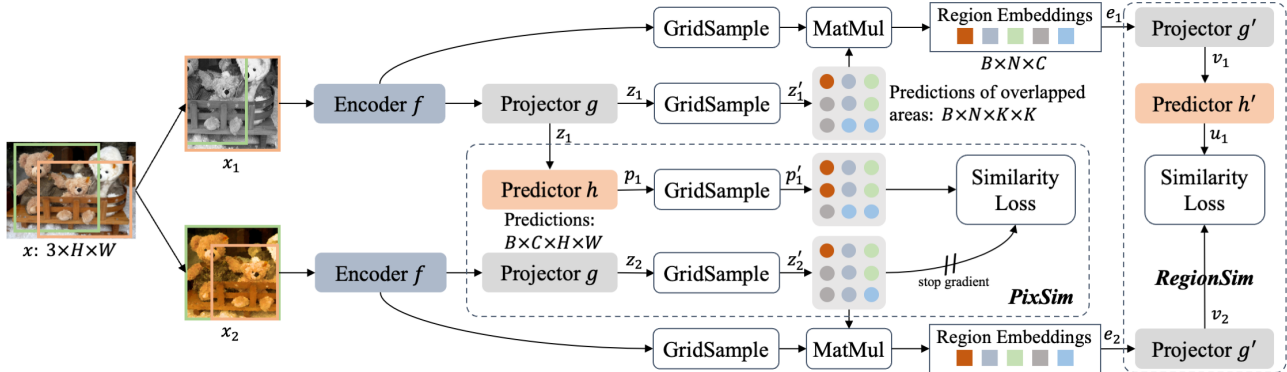


Figure 2. **Pipeline of DenseSiam.** DenseSiam takes two randomly augmented views of an image x as inputs. The two views are processed by an encoder network f without global average pooling (GAP), followed by a projector network g . The predictor network h transforms the dense prediction of the projector of one view. Then GridSample module samples the same pixels inside the intersected regions of the two views and interpolates their feature grids. The similarity between feature grids from two views are maximized by PixSim. Then DenseSiam multiplies the features of encoder and the dense predictions by projector g in the overlapped area to obtain region embeddings of each image. These region embeddings are processed by a new projector g' and new predictor h' for region level similarity learning.

mentation masks [24].

Unsupervised Semantic Segmentation. Unsupervised semantic segmentation aims to predict labels for each pixel without annotations. There are a few attempts that introduce heuristic masks and conduct similarity learning between segments (regions) [25, 44] with object-centric images. Most methods focus on natural scene images and exploit the assumption that semantic information should be invariant to photometric transformations and equivariant to geometric transformations no matter how the model predicts the labels, which is inherently consistent with the goal of unsupervised representation learning. However, these methods still rely on clustering [11, 27, 33] to predict the per-pixel labels and maximize the consistency of cluster assignments in different views of the image, which is cumbersome and difficult to be used for large-scale data.

DenseSiam conducts unsupervised semantic segmentation by adding a class-balanced cross entropy loss without clustering, significantly reduces the training costs and makes it scalable for large-scale data. RegionSim further boosts the segmentation accuracy by maximizing the consistency between regional features.

3. Dense Siamese Network

DenseSiam, as shown in Fig. 2, is a generic unsupervised learning framework for dense prediction tasks. The framework is inspired by SimSiam [10] but differs in its formulation tailored for learning dense representation (Sec. 3.1). In particular, it conducts dense similarity learning by PixSim (Sec. 3.2), which aims at maximizing pixel-level spatial consistency between grid sampled predictions. Based on the region embeddings derived from per-pixel predictions inferred in PixSim, DenseSiam further performs region-level contrastive learning through RegionSim (Sec. 3.3).

3.1. Siamese Dense Prediction

As shown in Fig. 2, DenseSiam takes two randomly augmented views x_1 and x_2 of an image x as inputs. The two views are processed by an encoder network f and a projector network g . The encoder network can either be a backbone network like ResNet-50 [23] or a combination of networks such as ResNet-50 with FPN [29]. As the encoder network f does not use global average pooling (GAP), the output of f is a *dense feature map* and is later processed by the projector g , which consists of three 1×1 convolutional layers followed by Batch Normalization (BN) and ReLU activation. Following the design in SimSiam [10], the last BN layer in g does not use learnable affine transformation [26]. The projector g projects the per-pixel embeddings to either a feature space for representation learning or to a labels space for segmentation. Given the dense prediction from g , noted as $z_1 \triangleq g(f(x_1))$, the predictor network h transforms the output of one view and matches it to another view [10]. Its output is denoted as $p_1 \triangleq h(g(f(x_1)))$.

The encoder and projector essentially form a Siamese architecture, which outputs two dense predictions (z_1 and z_2) for two views of an image, respectively. DenseSiam conducts similarity learning of different granularities using the Siamese dense predictions with the assistance of predictor [10, 19]. After unsupervised pre-training, only the encoder network is fine-tuned for downstream dense prediction tasks, where the projector is only used during pre-training to improve the representation quality [8]. When directly learning the dense prediction tasks, the encoder and projector are combined to tackle the task.

3.2. PixSim

Dense Similarity Learning. We formulate the dense similarity learning to maximize the similarity of dense predic-

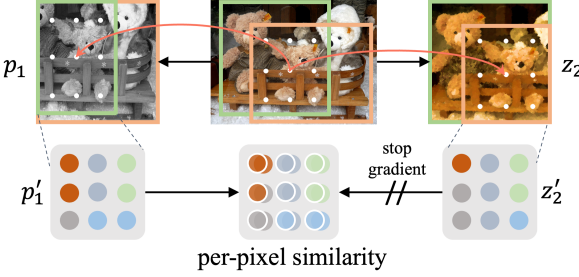


Figure 3. **Grid Sample module when grid size $K=3$.** Pixels at the same location in the original image should have similar predictions when they are transformed into two views. The Grid Sample module samples these pixels and interpolates their predictions in two views. The predictions of one view are learned to match those in another view.

tions inside the overlapping regions between p_1 and z_2 . Specifically, given the relative coordinates of the intersected region in x_1 and x_2 , we uniformly sample $K \times K$ point grids inside the intersected region from both views as shown in Fig. 3. These points in two views have exactly the same coordinates when they are mapped to the original image x ; thus, their predictions should be consistent to those in another view. Assuming the sampled feature grids are $z'_1 \triangleq \text{gridsample}(z_1)$ and $p'_1 \triangleq \text{gridsample}(p_1)$, PixSim minimizes the distance of the feature grids by a symmetrical loss [10, 19]:

$$\mathcal{L}_{dense} = \frac{1}{2} \mathcal{D}(p'_1, \text{stopgrad}(z'_2)) + \frac{1}{2} \mathcal{D}(p'_2, \text{stopgrad}(z'_1)), \quad (1)$$

where stopgrad is the stop-gradient operation to prevent feature ‘collapsing’ [10] and \mathcal{D} is a distance function that can have many forms [6, 10]. Two representative distance functions are negative cosine similarity [10, 19]

$$\mathcal{D}(p'_1, z'_2) = - \frac{p'_1}{\|p'_1\|_2} \cdot \frac{z'_2}{\|z'_2\|_2}, \quad (2)$$

and cross-entropy similarity

$$\mathcal{D}(p'_1, z'_2) = - \text{softmax}(p'_1) \cdot \log \text{softmax}(z'_2). \quad (3)$$

Advantages to Image-Level Similarity Learning. Previous formulation of image-level representation learning faces two issues when transferring their representations for dense prediction tasks. First, it learns global embeddings for each image during similarity learning, where most of the spatial information is discarded during GAP. Hence, the spatial consistency is not guaranteed in its goal of representation learning, while dense prediction tasks like semantic segmentation and object detection rely on the spatial information of each pixel. Second, it is common that p_1 and z_2 contain different contents (see examples of x_1 and x_2 in

Fig. 2) after heavy data augmentations like random cropping and resizing, but the global embeddings that encode these different contents are forced to be close to each other during training. This forcefully makes the embeddings of different pixel groups to be close to each other, breaking the regional consistency and is thus undesirable for dense prediction tasks. PixSim resolves the above-mentioned issues by conducting pixel-wise similarity learning inside the intersected regions of two views. Hence, DenseSiam can pre-train more favorable dense representations for dense prediction tasks.

3.3. RegionSim

When using cross-entropy with softmax as the training objective, PixSim implicitly groups similar pixels together into the same regions/segments. The consistency of such regions can be further maximized by the proposed RegionSim to learn better dense representation. The connection between PixSim and RegionSim is seamless - region-level similarity learning can be achieved without heuristic masks [24], saliency map [40], or manually cropping multiple regional features [37, 48, 49] as in previous studies.

Region Embedding Generation. As shown in Fig. 2, DenseSiam first obtains the feature grids of the intersected regions of each view by grid sampling from the features produced by the encoder f . This restricts RegionSim inside the intersected regions to ensure that the region embeddings to encode the similar contents. For simplicity, the region embeddings $e_1 \in \mathcal{R}^{N \times C}$ are obtained by the summation of multiplication between the masks and features as

$$e_1 = \sum_{i,j}^{K \times K} z'_1[i,j] \cdot \text{gridsample}(f(x_1))[i,j], \quad (4)$$

where N and C represent the number of sub-regions and the number of feature channels, respectively. The process yields an embedding for each segment of each pseudo category, which will then be used for contrastive learning to increase the consistency between these region embeddings.

Region Similarity Learning. After obtaining the region embeddings, RegionSim transforms them by a projector network g' , which is a three-layer MLP head [8, 10, 19]. The output of g' is then transformed by h' for contrasting or matching with another view. RegionSim assumes each region embedding of a sub-region to be consistent with the embedding of the sub-region in another view. Therefore, Eq. 1 can be directly applied to these region embeddings to conduct region-level similarity learning. Meanwhile, we also enforce the region embedding to have low similarities with the embeddings of other region embeddings to make the feature space more compact. Consequently, by denoting the two outputs as $u_1 \triangleq h'(g'(e_1))$ and $v_2 \triangleq g'(e_2)$, Region-

Sim can also minimize the symmetrized loss function

$$\mathcal{L}_{region} = \frac{1}{2}\mathcal{L}_c(u_1, v_2) + \frac{1}{2}\mathcal{L}_c(u_2, v_1). \quad (5)$$

The contrastive loss function [42] \mathcal{L}_c can be written as

$$\mathcal{L}_c(u_1, v_2) = - \sum_s^N \log \frac{\exp(u_1^s \cdot v_2^s)}{\sum_{s'}^N \exp(u_1^s \cdot v_2^{s'})}. \quad (6)$$

3.4. Learning Objective

When conducting unsupervised representation learning, DenseSiam also maintains a global branch to conduct image-level similarity learning to enhance the global consistency of representations, besides PixSim and RegionSim shown in Fig. 2. The architecture of the global branch remains the same as SimSiam [10]. The number of channels in the projector and predictor of PixSim is set to 512 for efficiency. The projector and predictor in RegionSim also use 512 channels. Denoting the loss of the global branch as \mathcal{L}_{sim} , DenseSiam optimizes the following loss

$$\mathcal{L} = \mathcal{L}_{sim} + \lambda_1 \mathcal{L}_{dense} + \lambda_2 \mathcal{L}_{region}, \quad (7)$$

where λ_1 and λ_2 are loss weights of \mathcal{L}_{dense} for PixSim and \mathcal{L}_{region} for RegionSim, respectively. The encoder f is used for fine-tuning in downstream dense prediction tasks after pre-training.

4. Unsupervised Semantic Segmentation

The proposed framework is appealing in that it can be readily extended to address dense prediction tasks such as unsupervised semantic segmentation, by simply adding a task-specific losses and layers, without needing the offline and cumbersome clustering process [11, 27, 33].

Formally, when using cross-entropy similarity (Eq. 3) in PixSim, the softmax output $\text{softmax}(z)$ can be regarded as the probabilities of belonging to each of N pseudo-categories. In such a case, the projector g predicts a label for each pixel, which aligns with the formulation for unsupervised semantic segmentation.

DenseSiam uses ResNet with a simplified FPN [11, 29] as the encoder g . The output channel N of PixSim is modified to match the number of classes in the dataset (e.g., 27 on COCO stuff-thing dataset [11, 30]). Our experiment shows that a direct change in the number of output channels in PixSim without any further modification can already yield reasonable performance without feature ‘collapsing’. Following previous method [11] that encourages the prediction scores to have a lower entropy (*i.e.*, more like one-hot scores), we add a cross entropy loss, denoted as \mathcal{L}_{seg} , when applying PixSim for unsupervised semantic segmentation with the pseudo labels obtained by $\text{argmax}(z_1)$.

We also observe that the small number of categories undermines the training stability, which is also a common issue in clustering-based methods [11, 27]. To solve this issue, DenseSiam introduces another set of projector and predictor in PixSim to keep a large number of pseudo categories following the over-clustering strategy [11, 27]. This head only conducts similarity learning using Eq. 1, noted as \mathcal{L}_{aux} . Therefore, the overall loss of DenseSiam for unsupervised semantic segmentation is calculated as

$$\mathcal{L} = \lambda_1 \mathcal{L}_{dense} + \lambda_2 \mathcal{L}_{region} + \lambda_3 \mathcal{L}_{seg} + \lambda_4 \mathcal{L}_{aux}. \quad (8)$$

We use $\lambda_4 = \frac{\log N}{\log N + \log N_{aux}}$ and $\lambda_1 = \frac{\log N_{aux}}{\log N + \log N_{aux}}$ to prevent the auxiliary loss from overwhelming the gradients because it uses a larger number N_{aux} of pseudo categories [11]. Note that RegionSim is only used in training to enhance the region consistency of dense labels predicted by PixSim. Only the encoder f and projector g are combined to form a segmentation model at inference time.

5. Experiments

5.1. Experimental Settings

Datasets. For unsupervised pre-training, we compare with other methods on ImageNet-1k [38] (IN1k) dataset and conduct ablation studies on COCO [30] dataset as it is smaller. COCO and IN1k are two large-scale datasets that contain $\sim 118K$ and ~ 1.28 million images, respectively. Though having more images, IN1k is highly curated and it mainly consists of object-centric images. Thus, the data is usually used for image classification. In contrast, COCO contains more diverse scenes in the real world and it has more objects (~ 7 objects *vs.* ~ 1 in IN1k) in one image. Hence, it is mainly used for dense prediction tasks like object detection, semantic, instance, and panoptic segmentation.

For unsupervised semantic segmentation, the model is trained and evaluated on curated subsets [11, 27] of COCO `train2017` split and `val2017` split, respectively. The training and validation set contain 49,629 images and 2,175 images, respectively. The semantic segmentation annotations include 80 thing categories and 91 stuff categories [4]. We follow previous methods [11, 27] to merge these categories to form 27 (15 ‘stuff’ and 12 ‘things’) categories.

Training Setup. We closely follow the pre-training settings of SimSiam [10] when conducting unsupervised pre-training experiments of DenseSiam. Specifically, we use a learning rate of $lr \times \text{BatchSize}/256$ following the linear scaling strategy [18], with a base $lr = 0.05$. We use the cosine decay learning rate schedule [32] and SGD optimizer, where the weight decay is 0.0001 and the SGD momentum is 0.9. The batch size is 512 by default. We pre-train DenseSiam for 800 epochs on COCO and for 200 epochs on IN1k. ResNet-50 [23] is used as default.

Table 2. **Transfer Learning.** All unsupervised methods are either based on 200-epoch pre-training in ImageNet (‘IN1k’). *COCO instance segmentation* and *COCO detection*: Mask R-CNN [22] (1× schedule) fine-tuned in COCO train2017; *Cityscapes*: FCN fine-tuned on Cityscapes dataset [13]; *VOC 07+12 detection*: Faster R-CNN fine-tuned on VOC 2007 trainval + 2012 train, evaluated on VOC 2007 test; COCO train2017, evaluated on COCO val2017. All Mask R-CNN are with FPN [29]. All Faster R-CNN models are with the C4-backbone [17]. All VOC and Cityscapes results are averaged over 5 trials

Pre-train	COCO Instance Seg.			COCO Detection			Cityscapes mIoU	VOC 07+12 Detection		
	AP ^{mask}	AP ₅₀ ^{mask}	AP ₇₅ ^{mask}	AP	AP ₅₀	AP ₇₅		AP	AP ₅₀	AP ₇₅
scratch	29.9	47.9	32.0	32.8	50.9	35.3	63.5	32.8	59.0	31.6
supervised	35.9	56.6	38.6	39.7	59.5	43.3	73.7	54.2	81.6	59.8
BYOL [19]	34.9	55.3	37.5	38.4	57.9	41.9	71.6	51.9	81.0	56.5
SimCLR [8]	34.8	55.2	37.2	38.5	58.0	42.0	73.1	51.5	79.4	55.6
MoCo v2 [9]	36.1	56.9	38.7	39.8	59.8	43.6	74.5	57.0	82.4	63.6
SimSiam [10]	36.4	57.4	38.8	40.4	60.4	44.1	76.3	56.7	82.3	63.4
ReSim [48]	36.1	56.7	38.8	40.0	59.7	44.3	76.8	58.7	83.1	66.3
DetCo [49]	36.4	57.0	38.9	40.1	60.3	43.9	76.5	57.8	82.6	64.2
DenseCL [45]	36.4	57.0	39.2	40.3	59.9	44.3	75.7	58.7	82.8	65.2
PixPro [50]	36.6	57.3	39.1	40.5	60.1	44.3	76.3	59.5	83.4	66.9
DenseSiam	36.8	57.6	39.8	40.8	60.7	44.6	77.0	58.5	82.9	65.3

For unsupervised semantic segmentation, for a fair comparison, we follow PiCIE [11] to adopt the backbone pre-trained on IN1k in a supervised manner. The backbone is then fine-tuned with DenseSiam for unsupervised semantic segmentation using the same base learning rate, weight decay, and SGD momentum as those used in unsupervised representation learning. The batch size is 256 by default. We empirically find the constant learning schedule works better so the learning rate is not altered during training. The model is trained for 10 epochs. ResNet-18 [23] is used as default for a fair comparison with previous methods [11].

Evaluation Protocol of Transfer Learning. For unsupervised pre-training, we evaluate the transfer learning performance of the pre-trained representations following Wang *et al.* [45]. We select different dense prediction tasks to comprehensively evaluate the transferability of the dense representation, including semantic segmentation, object detection, and instance segmentation. Challenging and popular dataset with representative algorithms in each task is selected.

When evaluating on semantic segmentation, we fine-tune a FCN [31] model and evaluate it with the Cityscapes dataset [13]. The model is trained on the `train_fine` set (2975 images) for 40k iterations and is tested on the `val` set. Strictly following the settings in MMSegmentation [12], we use FCN-D8 with a crop size of 769, a batch size of 16, and synchronized batch normalization. Results are averaged over five trials.

When evaluating on object detection, we fine-tune a Faster R-CNN [36] with C4-backbone by 24k iterations on VOC 2007 trainval + 2012 train set and is tested in VOC 2007 test set. Results are reported as an average over five trials.

We also evaluate the representation on object detection and instance segmentation on COCO dataset [30]. We fine-tune a Mask R-CNN with FPN [29] with standard multi-

scale 1x schedule [7, 46] on COCO train2017 split and evaluate it on COCO val2017 split. We apply synchronized batch normalization in backbone, neck, and ROI heads during training [21, 45].

Evaluation of Unsupervised Semantic Segmentation. Since the model is trained without labels, a mapping between the model’s label space and the ground truth categories needs be established. Therefore, we first let the model predicts on each image on the validation set, then we calculate the confusion matrix between the predicted labels and the ground truth classes. We use linear assignment to build a one-to-one mapping between the predicted labels and ground truth classes with the confusion matrix. Then we calculate mean IoU over all classes based on the obtained mapping [11, 27]. To more comprehensively understand the model’s behavior, we also report mean IoU of stuff and things classes, noted as mIoUSt and mIoUTh, respectively.

5.2. Transfer Learning Results

The comparison on transfer learning in dense prediction tasks between DenseSiam and previous unsupervised representation learning methods [8, 10, 19, 20, 45, 48] is shown in Table 2. The results of scratch, supervised, MoCo v2 [9], DenseCL [45], SimCLR [8], and BYOL [19] are reported from DenseCL [45]. For fair comparison, we fine-tune the model of ReSim-C4 [48] using the similar setting (Sec. 5.1). The model checkpoint is released by the paper authors¹. We report the results of SimSiam [10], DetCo [49], and PixPro [50] based on our re-implementation.

COCO Instance Segmentation and Detection. As shown in the first two columns of Table 2, DenseSiam outperforms SimSiam by 0.4 AP^{mask} on COCO instance segmentation. The improvements over SimSiam is on-par with that of

¹<https://github.com/Tete-Xiao/ReSim>

DenseCL and DetCo over MoCo v2 (0.4 *vs.* 0.3 AP^{mask}) and is better than ReSim (0.4 *vs.* 0 AP^{mask}). This further verifies the effectiveness of DenseSiam. Notably, DenseSiam outperforms ReSim, DetCo, DenseCL, and PixPro by 0.7, 0.4, 0.4, and 0.2 AP^{mask}, respectively. The results in COCO object detection is consistent with that in instance segmentation.

Cityscapes Semantic Segmentation. We compare DenseSiam with previous methods on semantic segmentation on Cityscapes dataset [13] and report the mean IoU (mIoU) of fine-tuned models. DenseSiam surpasses SimSiam by 0.7 mIoU and outperforms previous dense representation learning methods ReSim, DetCo, DenseCL, and PixPro by 0.2, 0.5, 1.3, and 0.7 mIoU, respectively. Notably, image-level unsupervised method such as SimCLR [8], BYOL [19] and SimSiam [10] show considerable performance gap against dense unsupervised methods including DenseSiam, DenseCL, and ReSim, indicating that pre-training with image-level similarity learning is sub-optimal for dense prediction tasks.

PASCAL VOC Object Detection. We further compare DenseSiam with previous methods on PASCAL VOC [16] object detection. We report the original metric AP₅₀ (AP calculated with IoU threshold 0.5) of VOC and further report COCO-style AP [46] and AP₇₅, which are stricter criteria in evaluating the detection performance. DenseSiam show a large improvement of 1.8 AP in comparison with SimSiam [10]. Notably, DenseSiam exhibits considerable improvements on AP₇₅ than AP₅₀, suggesting the effectiveness of DenseSiam in learning accurate spatial information. Its improvement over SimSiam is more than that of DetCo [49] (0.8 AP) over MoCo v2, and is on-par with those of DenseCL [45] and ReSim [48] over MoCo v2 [9].

DenseCL, ReSim, and PixPro are 0.2, 0.2, and 1.0 AP better than DenseSiam, respectively. This phenomenon contradicts the results in the benchmarks of COCO dataset, although their improvements over their image-level counterparts are consistent across benchmarks. We hypothesize that the different backbones used in the two benchmarks leads to this phenomenon, where ResNet-50-C4 backbone [36] is used on PASCAL VOC but ResNet-50-FPN [29] is used on COCO. The hypothesis also explains the inferior performance of DetCo [49]: DetCo conducts contrastive learning on pyramid features but only one feature scale is used when fine-tuning Faster R-CNN on PASCAL VOC dataset.

5.3. Unsupervised Segmentation Results

In Table 3 we compare DenseSiam with previous state-of-the-art methods in unsupervised semantic segmentation. DenseSiam achieves new state-of-the-art performance of 16.4 mIoU, surpassing PiCIE by 2 mIoU over all classes. Imbalanced performance is observed in previous meth-

Table 3. **Unsupervised Semantic Segmentation.** The model is trained and tested on the curated COCO dataset [11, 27]. ‘+ aux.’ denotes PiCIE or DenseSiam is trained with an auxiliary head

Method	mIoU	mIoU St	mIoU Th	Time (h)
Modified Deep Clustering [5]	9.8	22.2	11.6	-
IIC [27]	6.7	12.0	13.6	-
PiCIE [11] + aux.	14.4	17.3	23.8	18
DenseSiam + aux.	16.4	24.5	29.5	5

ods between thing and stuff classes, *e.g.*, PiCIE [11] and IIC [27] surpass Modified DeepClustering [5] on thing classes but fall behind on stuff classes. In contrast, DenseSiam consistently outperforms previous best results on both thing and stuff classes by more than 2 mIoU.

We also calculate the training costs of PiCIE and DenseSiam by measuring the GPU hours used to train the model with similar batch size and backbone. Because PiCIE needs clustering to obtain pseudo labels before each training epoch, its training time is comprised of the time of label clustering, data loading, and model’s forward and backward passes. In contrast, DenseSiam does not rely on clustering, its training time only consists of the time of data loading and forward/backward passes. In the setting of single GPU training, DenseSiam saves $\sim 72\%$ training costs in comparison with PiCIE.

5.4. Ablation Study

Unsupervised Pre-training. We ablate the key components in DenseSiam as shown in Table 4.

i) Effective grid number K in PixSim: We study the effective number K used in grid sampling in PixSim in Table 4a. The greater the number, the more feature grids will be sampled from the intersected regions and will be used for similarity learning. With zero grid number DenseSiam degenerates to the SimSiam baseline where no pixel similarity learning is performed. The results in Table 4a shows that 7×7 feature grids is sufficient to improve the per-pixel consistency of dense representation. We also compare the training memory used in PixSim. The comparison shows that PixSim only brings $0.1\% \sim 0.3\%$ extra memory cost in comparison with SimSiam.

ii) Loss weight of PixSim: We further study the loss weight λ_1 of \mathcal{L}_{dense} used for per-pixel similarity learning. The comparative results in Table 4b show that with $\lambda_1 = 1$ we achieve the best performance, which is equal to the loss weight of the image-level similarity learning.

iii) Orders of grid sample, projector, and predictor: As DenseSiam consists of encoder, projector, and predictor, we study the optimal position where the grid sampler should be introduced. The results in Table 4d show that it is necessary to put the grid sample module after the projector, but the predictor can perform equally well when it is before or behind the grid sample module.

Table 4. **Ablation studies in unsupervised pre-trainings.** All unsupervised representations are based on 800-epoch pre-training on COCO train2017. The representations are fine-tuned with Faster R-CNN [36] (C4-backbone) in VOC 2007 trainval + 2012 train and evaluated on VOC 2007 test. ‘Mem.’ indicates memory cost measured by Gigabyte (GB). The results of fine-tuning are averaged over 5 trials. Best settings are bolded and used as default settings

(a) The effective number K in PixSim

Gird Number	AP	AP ₅₀	AP ₇₅	Mem.
0	53.5	79.7	59.3	8.06
1	28.8	53.8	27.1	8.11
3	53.9	80.0	59.4	8.12
7	54.9	80.8	60.9	8.18
9	54.6	80.7	60.6	8.21
14	54.7	80.6	60.8	8.28

(b) The effective loss weight of PixSim

λ_1	AP	AP ₅₀	AP ₇₅
0	53.5	79.7	59.3
0.1	53.3	79.6	58.8
0.3	53.5	79.9	58.8
0.5	54.0	80.2	60.0
0.7	54.0	79.8	59.8
1.0	54.9	80.8	60.9

(c) The effective loss weight of RegionSim

λ_2	AP	AP ₅₀	AP ₇₅
0	53.5	79.7	59.3
0.01	55.3	81.0	61.3
0.05	55.0	80.9	60.6
0.1	55.5	81.1	61.5
0.2	55.3	81.0	61.0
0.5	55.3	80.9	61.1

(d) The effective order of grid sample, projector, and predictor in PixSim

Order	AP	AP ₅₀	AP ₇₅
-	53.5	79.7	59.3
grid. + proj. + pred.	53.4	79.6	59.0
proj. + grid. + pred.	54.7	80.6	60.4
proj. + pred. + grid.	54.9	80.8	60.9

(e) Regions to be focused in global branch. ‘in.’ indicates the intersected regions

Image-level	Pixel-level	AP	AP ₅₀	AP ₇₅
global	N/A	53.5	79.7	59.3
in.	N/A	0.0	0.0	0.0
global	in.	54.9	80.8	60.9
in.	in.	35.6	61.5	35.6

(f) Suitable start epoch of RegionSim

Start epoch	AP	AP ₅₀	AP ₇₅
never	54.9	80.8	60.9
0.4	37.7	64.8	38.4
0.5	55.5	81.1	61.5
0.6	55.0	80.8	60.4

Table 5. **Ablation study in unsupervised segmentation.** ‘Aux.’ indicates auxiliary head

PixSim	Aux.	CE	Region.	mIoU	mIoU St	mIoU Th
✓				10.1	19.0	17.7
✓	✓			11.1	20.4	22.3
✓	✓	✓		15.0	24.8	23.4
✓	✓	✓	✓	16.4	24.5	29.5

iv) *Regions to focus in global branch:* We also study the regions that should be focused in global branch in Table 4e, as an image-level similarity learning branch (SimSiam) is kept to facilitate training. The abbreviations ‘global’ and ‘in.’ indicate whether the similarity learning is conducted with the whole image or the intersected regions between two views. To maximize per-pixel consistency, PixSim is always conducted with the intersected regions. We find that the focusing on the whole image when conducting image-level similarity learning is always important in both SimSiam and DenseSiam. Only using the intersected regions will lead to feature ‘collapsing’ (second row with zero accuracy in downstream tasks) in SimSiam.

v) *Loss weight of RegionSim:* We study the loss weight λ_2 of RegionSim as shown in Table 4c. We find that 0.1 works best and large value of λ_2 leads decreased performance.

vi) *Start point of RegionSim:* The start point of RegionSim matters. The label prediction quality is not accurate and may lead to a wrong optimization direction if RegionSim is applied at a wrong time. Starting RegionSim at the middle point of training yields the best performance.

Unsupervised Semantic Segmentation. We also study the effectiveness of the components in DenseSiam for unsupervised semantic segmentation. Directly applying PixSim without any further modification yields 10.1 mIoU, which already surpasses many previous methods [5, 27] (9.8 and 6.7 mIoU). Adding CE loss further improves the performance by making the feature space more compact and discriminative. After adding the auxiliary head, the model al-

Table 6. **Analysis:** Strategies for building visual correspondence

Strategies	AP	AP ₅₀	AP ₇₅
SimSiam	53.5	79.7	59.3
feature similarity [45]	36.3	63.5	36.1
pixel distance [50]	53.7	79.3	58.5
candidate regions [37, 48]	54.7	79.9	60.5
location	54.9	80.8	60.9
location + region embeddings	55.5	81.1	61.5

ready surpasses the previous state-of-the-art method PiCIE. RegionSim further brings 1.4 mIoU of improvement.

Exploitation of Correspondence. Previous methods explore different strategies to build and optimize dense correspondence between two views. DenseCL [45] compares feature similarity to build the correspondence between pixels. PixPro [50] connects pixels by the distance of their coordinates in the original image. There are also attempts [37, 48] to use manual crops and maximize the similarity between similar crops in different views. DenseSiam uses the location and regions for similarity learning of different granularities. We study these strategies under the same architecture of PixSim with a switch between strategies. The results in Table 6 show that using feature similarity [45] significantly decreases the performance. This is because PixSim does not use negative pixel pairs, a prerequisite for the strategy to work. The strategy of using pixel coordinates only brings marginal improvements. Using location correspondence in PixSim is much simpler and more effective than candidate regions. DenseSiam yields the best results by exploiting the correspondence built with both location and region embeddings.

6. Conclusion

Different dense prediction tasks essentially shares the similar goal of optimizing the spatial consistency between views of images. DenseSiam exploits such a property and unanimously solves unsupervised dense representation

learning and unsupervised semantic segmentation within a Siamese architecture. DenseSiam optimizes similarity between dense predictions at pixel level by PixSim and at region level by RegionSim, with neither negative pixel pairs, momentum encoder, manual region crops, nor heuristic masks. DenseSiam pre-trains dense representations with competitive performance in downstream tasks. Its unsupervised semantic segmentation performance also achieves the new state-of-the-art.

A. Implementation Details

Data Augmentation. We use the same data augmentation techniques as those used in previous methods for a fair comparison.

i) Unsupervised pre-training: We use existing augmentation modules in PyTorch [34] and describe them using the same notations as the following. Specifically, for geometric augmentation, we use `RandomResizedCrop` with scale in [0.2,1.0] and `RandomHorizontalFlip`. For color augmentations we use `ColorJitter` and `RandomGrayscale` with probabilities of 0.8 and 0.2, respectively. The jittering strength of brightness, contrast, saturation, and hue are 0.4, 0.4, 0.4, and 0.1 in `ColorJitter`, respectively. Blurring augmentation [8] is also applied using a Gaussian kernel with std in [0.1, 2.0]. These hyper-parameters are the same as those adopted in previous methods [8–10, 19, 45].

i) Unsupervised semantic segmentation: We apply the same augmentations as those used in PiCIE [11] in unsupervised semantic segmentation for a fair comparison. The augmentations include color jittering, gray scale, blurring, cropping, and flipping. The color jittering augmentations consists of jittering brightness, contrast, saturation, and hue. These jittering transformations are randomly applied with probabilities of 0.8 with strength of 0.3, 0.3, 0.3, and 0.1, respectively. The gray scale augmentation is randomly applied with a probability of 0.2. Random crop is used with scale in [0.5,1.0]. Different from those augmentations used in unsupervised pre-training, the augmentations are sampled first and replayed with similar parameters in each epoch following PiCIE [11].

Exploitation of Correspondence. In Table 6 of the main paper, we compare different strategies of finding corresponding pixels between views. For a fair comparison, we keep the same architecture and symmetrized loss of PixSim and implement these strategies strictly following their official code releases. PixSim uses grid sample module to interpolate embeddings of pixels that have the same locations in the original image. To study feature similarity used in DenseCL [45], we calculate feature similarities between pixels and link the most similar pixels between views. To study pixel distance used in PixPro [50], we calculate the coordinate distances of pixels and link the pixels having

the close locations. To study candidate regions used in ReSim [48], we use anchors in the intersected regions generated by sliding windows.

The results show that location correspondence in PixSim exhibits superior performance than previous strategies in the simple dense Siamese architecture. Location correspondence is also much simpler and more effective than candidate regions. DenseSiam yields the best results by exploiting the correspondence built with both location and region embeddings.

References

- [1] Philip Bachman, R. Devon Hjelm, and William Buchwalter. Learning representations by maximizing mutual information across views. In Hanna M. Wallach, Hugo Larochelle, Alina Beygelzimer, Florence d’Alché-Buc, Emily B. Fox, and Roman Garnett, editors, *NeurIPS*, 2019. 2
- [2] Luca Bertinetto, Jack Valmadre, João F. Henriques, Andrea Vedaldi, and Philip H. S. Torr. Fully-convolutional siamese networks for object tracking. In *ECCV*, 2016. 2
- [3] Jane Bromley, James W Bentz, Léon Bottou, Isabelle Guyon, Yann LeCun, Cliff Moore, Eduard Säckinger, and Roopak Shah. Signature verification using a “siamese” time delay neural network. In *NeurIPS*, 1993. 2
- [4] Holger Caesar, Jasper Uijlings, and Vittorio Ferrari. COCO-Stuff: Thing and stuff classes in context. In *CVPR*, 2018. 5
- [5] Mathilde Caron, Piotr Bojanowski, Armand Joulin, and Matthijs Douze. Deep clustering for unsupervised learning of visual features. In *ECCV*, 2018. 1, 2, 7, 8
- [6] Mathilde Caron, Ishan Misra, Julien Mairal, Priya Goyal, Piotr Bojanowski, and Armand Joulin. Unsupervised learning of visual features by contrasting cluster assignments. In *NeurIPS*, 2020. 1, 2, 4
- [7] Kai Chen, Jiaqi Wang, Jiangmiao Pang, Yuhang Cao, Yu Xiong, Xiaoxiao Li, Shuyang Sun, Wansen Feng, Ziwei Liu, Jiarui Xu, Zheng Zhang, Dazhi Cheng, Chenchen Zhu, Tianheng Cheng, Qijie Zhao, Buyu Li, Xin Lu, Rui Zhu, Yue Wu, Jifeng Dai, Jingdong Wang, Jianping Shi, Wanli Ouyang, Chen Change Loy, and Dahua Lin. MMDetection: Open mmlab detection toolbox and benchmark. *arXiv preprint arXiv:1906.07155*, 2019. 6
- [8] Ting Chen, Simon Kornblith, Mohammad Norouzi, and Geoffrey E. Hinton. A simple framework for contrastive learning of visual representations. In *ICML*, 2020. 1, 2, 3, 4, 6, 7, 9
- [9] Xinlei Chen, Haoqi Fan, Ross B. Girshick, and Kaiming He. Improved baselines with momentum contrastive learning. *CoRR*, abs/2003.04297, 2020. 2, 6, 7, 9
- [10] Xinlei Chen and Kaiming He. Exploring simple siamese representation learning. In *CVPR*, 2021. 1, 2, 3, 4, 5, 6, 7, 9
- [11] Jang Hyun Cho, Utkarsh Mall, Kavita Bala, and Bharath Hariharan. PiCIE: Unsupervised semantic segmentation using invariance and equivariance in clustering. In *CVPR*, 2021. 1, 2, 3, 5, 6, 7, 9

[12] MMSegmentation Contributors. MMSegmentation: Openmmlab semantic segmentation toolbox and benchmark. <https://github.com/open-mmlab/mmsegmentation>, 2020. 6

[13] Marius Cordts, Mohamed Omran, Sebastian Ramos, Timo Rehfeld, Markus Enzweiler, Rodrigo Benenson, Uwe Franke, Stefan Roth, and Bernt Schiele. The cityscapes dataset for semantic urban scene understanding. In *CVPR*, 2016. 6, 7

[14] Zhigang Dai, Bolun Cai, Yugeng Lin, and Junying Chen. UP-DETR: unsupervised pre-training for object detection with transformers. In *CVPR*, 2021. 2

[15] Alexey Dosovitskiy, Philipp Fischer, Jost Tobias Springenberg, Martin A. Riedmiller, and Thomas Brox. Discriminative unsupervised feature learning with exemplar convolutional neural networks. *TPAMI*, 2016. 2

[16] Mark Everingham, Luc Van Gool, Christopher K. I. Williams, John M. Winn, and Andrew Zisserman. The pascal visual object classes (VOC) challenge. *IJCV*, 2010. 7

[17] Ross Girshick, Ilya Radosavovic, Georgia Gkioxari, Piotr Dollár, and Kaiming He. Detectron. <https://github.com/facebookresearch/detectron>, 2018. 6

[18] Priya Goyal, Piotr Dollár, Ross B. Girshick, Pieter Noordhuis, Lukasz Wesolowski, Aapo Kyrola, Andrew Tulloch, Yangqing Jia, and Kaiming He. Accurate, large minibatch SGD: training imagenet in 1 hour. *CoRR*, abs/1706.02677, 2017. 5

[19] Jean-Bastien Grill, Florian Strub, Florent Altché, Corentin Tallec, Pierre H. Richemond, Elena Buchatskaya, Carl Doersch, Bernardo Ávila Pires, Zhaohan Guo, Mohammad Gheshlaghi Azar, Bilal Piot, Koray Kavukcuoglu, Rémi Munos, and Michal Valko. Bootstrap your own latent - A new approach to self-supervised learning. In *NeurIPS*, 2020. 1, 2, 3, 4, 6, 7, 9

[20] Kaiming He, Haoqi Fan, Yuxin Wu, Saining Xie, and Ross B. Girshick. Momentum contrast for unsupervised visual representation learning. In *CVPR*, 2020. 1, 2, 6

[21] Kaiming He, Ross Girshick, and Piotr Dollar. Rethinking ImageNet pre-training. In *ICCV*, 2019. 6

[22] Kaiming He, Georgia Gkioxari, Piotr Dollár, and Ross B. Girshick. Mask R-CNN. In *ICCV*, 2017. 6

[23] Kaiming He, Xiangyu Zhang, Shaoqing Ren, and Jian Sun. Deep residual learning for image recognition. In *CVPR*, 2016. 3, 5, 6

[24] Olivier J. Hénaff, Skanda Koppula, Jean-Baptiste Alayrac, Aäron van den Oord, Oriol Vinyals, and João Carreira. Efficient visual pretraining with contrastive detection. In *ICCV*, 2021. 1, 2, 3, 4

[25] Jyh-Jing Hwang, Stella X. Yu, Jianbo Shi, Maxwell D. Collins, Tien-Ju Yang, Xiao Zhang, and Liang-Chieh Chen. Segsort: Segmentation by discriminative sorting of segments. In *ICCV*, 2019. 3

[26] Sergey Ioffe and Christian Szegedy. Batch normalization: Accelerating deep network training by reducing internal covariate shift. In *ICML*, 2015. 3

[27] Xu Ji, Andrea Vedaldi, and João F. Henriques. Invariant information clustering for unsupervised image classification and segmentation. In *ICCV*, 2019. 1, 2, 3, 5, 6, 7, 8

[28] Gregory Koch, Richard Zemel, Ruslan Salakhutdinov, et al. Siamese neural networks for one-shot image recognition. In *ICML deep learning workshop*, 2015. 2

[29] Tsung-Yi Lin, Piotr Dollár, Ross B. Girshick, Kaiming He, Bharath Hariharan, and Serge J. Belongie. Feature pyramid networks for object detection. In *CVPR*, 2017. 3, 5, 6, 7

[30] Tsung-Yi Lin, Michael Maire, Serge Belongie, James Hays, Pietro Perona, Deva Ramanan, Piotr Dollár, and C Lawrence Zitnick. Microsoft COCO: Common objects in context. In *ECCV*, 2014. 5, 6

[31] Jonathan Long, Evan Shelhamer, and Trevor Darrell. Fully convolutional networks for semantic segmentation. In *CVPR*, 2015. 6

[32] Ilya Loshchilov and Frank Hutter. SGDR: stochastic gradient descent with warm restarts. In *ICLR*, 2017. 5

[33] Yassine Ouali, Céline Hudelot, and Myriam Tami. Autoregressive unsupervised image segmentation. In *ECCV*, 2020. 1, 3, 5

[34] Adam Paszke, Sam Gross, Soumith Chintala, Gregory Chanan, Edward Yang, Zachary DeVito, Zeming Lin, Alban Desmaison, Luca Antiga, and Adam Lerer. Automatic differentiation in PyTorch. In *NIPS Autodiff Workshop*, 2017. 9

[35] Pedro O. Pinheiro, Amjad Almahairi, Ryan Y. Benmalek, Florian Golemo, and Aaron C. Courville. Unsupervised learning of dense visual representations. In *NeurIPS*, 2020. 1, 2

[36] Shaoqing Ren, Kaiming He, Ross Girshick, and Jian Sun. Faster R-CNN: Towards real-time object detection with region proposal networks. In *NeurIPS*, 2015. 6, 7, 8

[37] Byungseok Roh, Wuhyun Shin, Ildoo Kim, and Sungwoong Kim. Spatially consistent representation learning. In *CVPR*, 2021. 1, 2, 4, 8

[38] Olga Russakovsky, Jia Deng, Hao Su, Jonathan Krause, Sanjeev Satheesh, Sean Ma, Zhiheng Huang, Andrej Karpathy, Aditya Khosla, Michael Bernstein, Alexander C. Berg, and Li Fei-Fei. ImageNet Large Scale Visual Recognition Challenge. *IJCV*, 2015. 5

[39] Florian Schroff, Dmitry Kalenichenko, and James Philbin. Facenet: A unified embedding for face recognition and clustering. In *CVPR*, 2015. 2

[40] Ramprasaath R. Selvaraju, Karan Desai, Justin Johnson, and Nikhil Naik. CASTing your model: Learning to localize improves self-supervised representations. In *CVPR*, 2021. 1, 2, 4

[41] Yaniv Taigman, Ming Yang, Marc’Aurelio Ranzato, and Lior Wolf. DeepFace: Closing the gap to human-level performance in face verification. In *CVPR*, 2014. 2

[42] Aäron van den Oord, Yazhe Li, and Oriol Vinyals. Representation learning with contrastive predictive coding. *CoRR*, abs/1807.03748, 2018. 5

[43] Wouter Van Gansbeke, Simon Vandenhende, Stamatios Georgoulis, Marc Proesmans, and Luc Van Gool. Scan: Learning to classify images without labels. In *ECCV*, 2020. 2

[44] Wouter Van Gansbeke, Simon Vandenhende, Stamatios Georgoulis, and Luc Van Gool. Unsupervised semantic seg-

mentation by contrasting object mask proposals. In *ICCV*, 2021. 3

[45] Xinlong Wang, Rufeng Zhang, Chunhua Shen, Tao Kong, and Lei Li. Dense contrastive learning for self-supervised visual pre-training. In *CVPR*, 2021. 1, 2, 6, 7, 8, 9

[46] Yuxin Wu, Alexander Kirillov, Francisco Massa, Wan-Yen Lo, and Ross Girshick. Detectron2. <https://github.com/facebookresearch/detectron2>, 2019. 6, 7

[47] Zhirong Wu, Yuanjun Xiong, Stella X. Yu, and Dahua Lin. Unsupervised feature learning via non-parametric instance discrimination. In *CVPR*, 2018. 2

[48] Tete Xiao, Colorado J. Reed, Xiaolong Wang, Kurt Keutzer, and Trevor Darrell. Region similarity representation learning. In *ICCV*, 2021. 1, 2, 4, 6, 7, 8, 9

[49] Enze Xie, Jian Ding, Wenhui Wang, Xiaohang Zhan, Hang Xu, Zhenguo Li, and Ping Luo. DetCo: Unsupervised contrastive learning for object detection. In *ICCV*, 2021. 1, 2, 4, 6, 7

[50] Zhenda Xie, Yutong Lin, Zheng Zhang, Yue Cao, Stephen Lin, and Han Hu. Propagate yourself: Exploring pixel-level consistency for unsupervised visual representation learning. In *CVPR*, 2021. 1, 2, 6, 8, 9

[51] Ceyuan Yang, Zhirong Wu, Bolei Zhou, and Stephen Lin. Instance localization for self-supervised detection pretraining. In *CVPR*, 2021. 1, 2

[52] Xiaohang Zhan, Jiahao Xie, Ziwei Liu, Yew-Soon Ong, and Chen Change Loy. Online deep clustering for unsupervised representation learning. In *CVPR*, 2020. 2